metals

MDPI

Article

The Improvement of Dehydriding the Kinetics of $NaMgH_3$ Hydride via Doping with Carbon Nanomaterials

Zhong-Min Wang *, Song Tao, Jia-Jun Li, Jian-Qiu Deng, Huaiying Zhou and Qingrong Yao

School of Material Science and Engineering, Guilin University of Electronic Technology, Guilin 541004, China; taosongaa@163.com (S.T.); ljjdzn@hotmail.com (J.-J.L.); jqdeng@guet.edu.cn (J.-Q.D.); zhy@guet.edu.cn (H.Z.); qingry96@guet.edu.cn (Q.Y.)

* Correspondence: zmwang@guet.edu.cn; Tel.: +86-773-2291956

Academic Editor: Jacques Huot

Received: 21 October 2016; Accepted: 23 December 2016; Published: 30 December 2016

Abstract: $NaMgH_3$ perovskite hydride and $NaMgH_3$–carbon nanomaterials (NH-CM) composites were prepared via the reactive ball-milling method. To investigate the catalytic effect of CM on the dehydriding kinetic properties of $NaMgH_3$ hydride, multiwall carbon nanotubes (MWCNTs) and graphene oxide (GO) were used as catalytic additives. It was found that dehydriding temperatures and activation energies (ΔE_1 and ΔE_2) for two dehydrogenation steps of $NaMgH_3$ hydride can be greatly reduced with a 5 wt. % CM addition. The NH–2.5M–2.5G composite presents better dehydriding kinetics, a lower dehydriding temperature, and a higher hydrogen-desorbed amount (3.64 wt. %, 638 K). ΔE_1 and ΔE_2 can be reduced by about 67 kJ/mol and 30 kJ/mol, respectively. The results suggest that the combination of MWCNTs and GO is a better catalyst as compared to MWCNTs or GO alone.

Keywords: $NaMgH_3$ hydride; doping; carbon nanomaterial (CM) composite; catalytic effect; dehydriding kinetics

1. Introduction

Perovskite-type hydride, $NaMgH_3$, as a potential candidate for on-board applications, has received considerable attention for its high gravimetric and volumetric hydrogen densities (6 wt. % and 88 kg/m^3, respectively), as well as its reversible hydriding and dehydriding reactions [1–7]. $NaMgH_3$ is characterized by an orthorhombic perovskite structure comprising [MgH_6] octahedra and [NaH_{12}] cubo-octahedra, which is analogous to $GdFeO_3$-type perovskite (space group Pnma). This space group is typical for low-tolerance-factor oxide perovskites, where the singly charged Na cation occupies eight-fold coordinated voids [8]. Sheppard et al. [9] reported the desorption enthalpy and entropy are 86.6 ± 1.0 kJ/(mol·H_2) and 132.2 ± 1.3 kJ/(mol·H_2) for the decomposition of $NaMgH_3$ into NaH and Mg, respectively, indicating that $NaMgH_3$ is thermodynamically more stable than magnesium hydride (MgH_2). One of the most promising approaches to improve its poor dehydrogenation property is incorporating with other metals or complex hydrides (e.g., $Na_{1-x}Li_xMgH_3$ [10–12], $NaMgH_3$-g-C_3N_4 [13], and $NaMgH_3$-MgH_2 [14,15]).

The addition of small amounts of catalytic material (transition metals, carbon materials, etc.) to MgH_2 has successfully reduced the time taken to absorb or desorb hydrogen [16–22]. Recently, carbon nanomaterials have been investigated as catalytic materials for enhancing the uptake and release of hydrogen from MgH_2 due to its lightweight nature. Alsabawi et al. [23] investigated the catalytic effect of up to 10 wt. % carbon buckyballs (C_{60}) on the kinetics of hydrogen desorption and the subsequent absorption of MgH_2. They found that a 1–2 wt. % C_{60} additive with 2 h of milling time are the optimum conditions for the best desorption kinetics. Imamura et al. reported the

enhanced kinetics of a ball-milled Mg–graphite composite with organic additives (tetrahydrofuran, cyclohexane, or benzene), and Raman characterization indicated that the organic additives allowed the graphite to shear along planes rather than grind into small particles, as it did without organic additives [24,25]. Thiangviriya et al. showed that the improvement of dehydrogenation kinetics of the $2LiBH_4$–MgH_2 composite by doping with activated carbon nanofibers is due to the increase in the hydrogen diffusion pathway and thermal conductivity [26]. Kadri et al. demonstrated that the presence of both a V-based catalyst and carbon nanotubes reduces the enthalpy and entropy of MgH_2, and partially destroyed CNTs are better at enhancing the hydrogen sorption performance [27]. Other forms of carbon, such as amorphous carbon [28,29], carbon black [28,30], activated carbons [31,32], and carbon nanotubes [28,33–39], have also been studied for their catalytic effect on the magnesium hydrogen system. $NaMgH_3$ can be synthesized via reactive mechanochemical means. Indeed, mechanochemical approaches provide not only less energy intensive routes to the hydrides, but also ensure that particles sizes are minimized, improving the dehydrogenation kinetics of the ternary hydrides compared to those prepared at high temperature [10,40].

In this work, multiwall carbon nanotubes (MWCNTs) and graphite (G) were used as catalytic additives. The reactive ball-milling method was employed to prepare $NaMgH_3$ perovskite hydride and $NaMgH_3$-carbon nanomaterials (NH-CM) composites. The effects of different additives on the structure, thermal stability, and dehydriding kinetic properties of $NaMgH_3$ hydride were investigated.

2. Materials and Methods

All sample handlings were undertaken in an argon atmosphere glovebox (Mbraun, Labstar, 1 ppm H_2O, 1 ppm O_2). $NaMgH_3$ hydride was prepared by reactive milling of stoichiometric mixtures of MgH_2 (>98% purity, Alfa-Aesar, Ward Hill, MA, USA) and NaH (99.9% purity, Sigma-Aldrich, Billerica, MA, USA). The mixed powders were milled with stainless steel balls, with a ball-to-powder weight ratio of 80:1, under a H_2 atmosphere (0.8 MPa) for 45 h at 320 rpm using a QM-3SP2 planetary mill at ambient temperature. Multiwall carbon nanotubes (MWCNTs, tube length: 0.5–2 μm, tube diameter: 30–50 nm, >95% purity, Chengdu Organic Chemistry Co., Ltd., Chengdu, China) and graphene oxide (GO, <10 sheets, >95% purity, Chengdu Organic Chemistry Co., Ltd., Chengdu, China) were introduced to $NaMgH_3$ hydride as catalysts. NH-CM composites were prepared by reactive milling the mixture of MgH_2, NaH, and catalytic additives under the same milling conditions. The composites of $NaMgH_3$ with different loading of carbon nanomaterials were labeled as follows: NH–5M ($NaMgH_3$ + 5 wt. % MWCNT composite), NH–5G ($NaMgH_3$ + 5 wt. % GO composite), and NH–2.5M–2.5G ($NaMgH_3$ + 2.5 wt. % MWCNTs + 2.5 wt. % G composite).

X-ray diffraction (XRD) samples were prepared in a glove box. To avoid exposure to air during the measurement, the sample was spread uniformly on the sample holder and covered with Scotch tape. XRD analysis was performed on Empyrean PIXcel 3D (PANalytical B.V., Almelo, The Netherlands) (Cu Kα radiation) with a scanning speed of 5°/min. The mean crystallite size was determined by the Scherer formula ($D = k\lambda/(\beta\_(hkl)\cos\theta)$), where D is the crystallite size, k is the shape factor (0.89), λ is the wavelength of the Cu Kα radiation (0.154056 nm), β_hkl is the FWHM (full width of peak at half maximum), and θ is the diffraction angle. The evaluations of the hydrogen-desorbed amount and the dehydriding kinetic properties of the samples were carried out in an automatic Sievert-type apparatus (PCTpro2000, Setaram Co., Caluire, France). Thermal properties of the $NaMgH_3$ and NH-CM composites were investigated by differential scanning calorimetry (DSC, NETZSCH STA 449F3, Selb, Germany) at different ramping rates (5, 10, and 15 K/min) under a continuous argon flow (20 mL/min) from 298 K to 725 K. The sample was loaded into an alumina crucible in the glove box. The crucible was then placed in a sealed glass bottle in order to prevent oxidation during transportation from the glove box to the TGA/DSC apparatus. An empty alumina crucible was used as a reference.

3. Results and Discussion

3.1. Structure Characterization of As-Prepared $NaMgH_3$ Hydride and NH-CM Composites

Figure 1 shows the XRD patterns of as-prepared $NaMgH_3$ hydride and NH-CM composites (NH–5M, NH–5G, and NH–2.5M–2.5G). The red long string is the standard line of $NaMgH_3$ phase. As can been seen, typical peaks of $NaMgH_3$ phase can be observed in all samples, which indicate an orthorhombic perovskite structure, similar to those of the $GdFeO_3$ type perovskite (space group Pnma) [41,42]. The sharp peaks are more prominent for $NaMgH_3$ hydride without a catalyst addition. A slight peak shift to a lower angle also is observed in these NH-CM composites. The calculated crystallite size are 15.8 nm for the as-synthesized $NaMgH_3$ sample, 14.9 nm for the NH–5M sample, 14.0 nm for the NH–5G sample, and 13.4 nm for the NH–2.5M–2.5G sample, respectively. The results indicate that the addition of 5 wt. % catalyst will reduce the crystallite size, which may improve dehydriding kinetics. The peaks of the catalysts are absent, probably because only a small amount of CM were added to the composites, and these additives were appeared in the form of an amorphous phase after ball-milling [11]. The existence of MgO can be attributed to the slight oxidization of samples in the handling process [43].

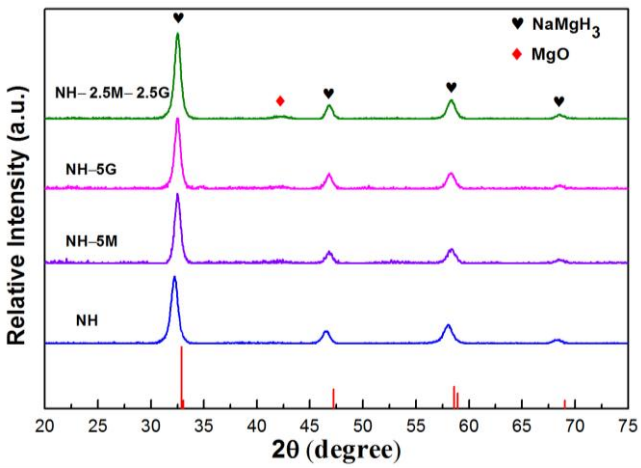

Figure 1. The XRD patterns of as-prepared $NaMgH_3$ hydride and NH-CM composites.

3.2. Thermal Stabilities of $NaMgH_3$ Hydride and NH-CM Composites

Figure 2 presents the DSC curves of $NaMgH_3$ hydride and three NH-CM composites at different heating rates (5, 10, and 20 K/min) under a continuous argon flow from 298 K to 750 K, where T_x and T_p represent the start and peak temperature of dehydrogenation, respectively. From the DSC curves, there are two endothermic peaks for all four samples, which are related to two decomposition steps of $NaMgH_3$ hydride. The decomposition steps can be expressed as follows [2]:

$$NaMgH_3 \rightarrow NaH + Mg + H_2\uparrow \quad (1)$$

$$NaH \rightarrow Na + \frac{1}{2}H_2\uparrow \quad (2)$$

In comparison with $NaMgH_3$ hydride without a catalyst addition, an obvious decrease of dehydriding temperature is observed in all composites. At a heating rate of 5 K/min, NH–2.5M–2.5G has the largest dehydriding temperatures reduction with temperature difference values of ΔT_{x1}, ΔT_{p1}, ΔT_{x2}, and ΔT_{p2} are 52.2 K, 51.1 K, 44.1 K, and 20.4 K, respectively. The next sample with the biggest reduction temperature differences was NH–5G, followed by NH–5M.

In order to estimate the dehydriding activation energy (ΔE) of $NaMgH_3$ hydride, the Kissinger plot is used for non-isothermal DSC analysis and can be expressed in the form as follows [44]:

$$\ln (T^2/\upsilon) = \Delta E/RT + \ln (\Delta E/Ru_0) \quad (3)$$

where T is the peak temperature, R is the gas constant (8.3145 J/(K·mol)), and υ and u_0 are the heating rate and frequency factor, respectively.

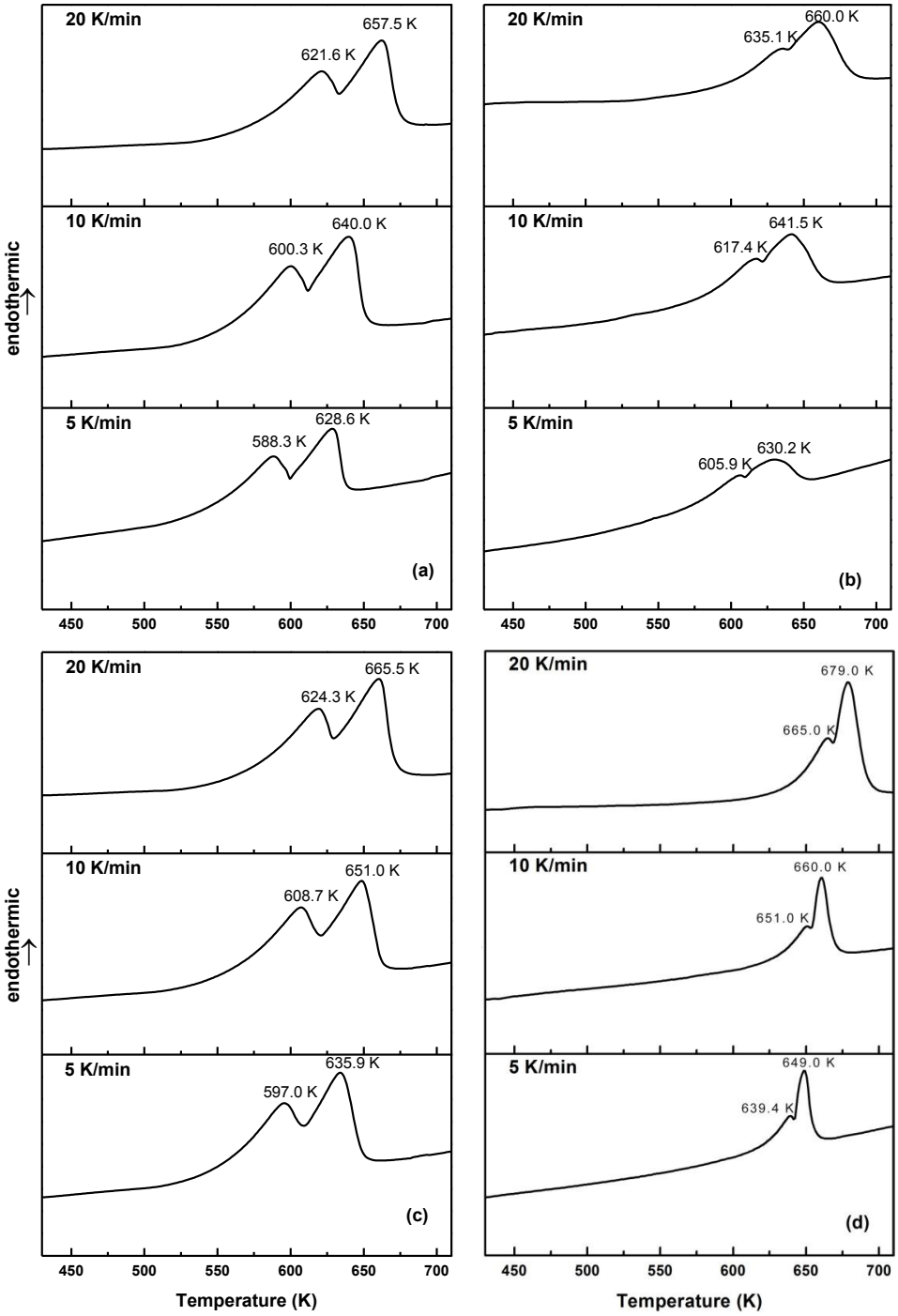

Figure 2. DSC curves of $NaMgH_3$ hydride and NH-CM composites at different heating rates. (**a**) NH–2.5M–2.5G; (**b**) NH–5G; (**c**) NH–5M; (**d**) $NaMgH_3$ hydride.

In Figure 3, both datasets at T_x and T_p show a good linear relation between ln (T^2/υ) and $(1000/T)$ with a slope of $\Delta E/R$. The calculated ΔE values are listed in Table 1. An obvious decrease of ΔE for both dehydrogenation steps of $NaMgH_3$ hydride is observed for those samples milled with the CM additive. The calculated ΔE_1 (the first decomposition step) and ΔE_2 (the second decomposition step) are 113.8 kJ/mol and 126.6 kJ/mol for the NH–2.5M–2.5G sample, 139.8 kJ/mol and 147.6 kJ/mol for the NH–5G sample, and 146.4 kJ/mol and 153.9 kJ/mol for the NH–5M sample, respectively. In comparison with $NaMgH_3$ hydride without a CM addition (ΔE_1 = 180.3 kJ/mol, ΔE_2 = 156.2 kJ/mol), the NH–2.5M–2.5G sample has the highest reduction of activation energy, ΔE, where the deviation values of ΔE_1 and ΔE_2 are about 67 kJ/mol and 30 kJ/mol, respectively. The results indicate that the activation energy (ΔE) for the dehydrogenation steps of the $NaMgH_3$ hydride can be greatly decreased by milling with a 5 wt. % CM addition, especially in the case of the NH–2.5M–2.5G composite. These observations correspond well with the DSC results, such that the dehydriding temperatures are lowered by the activation energy.

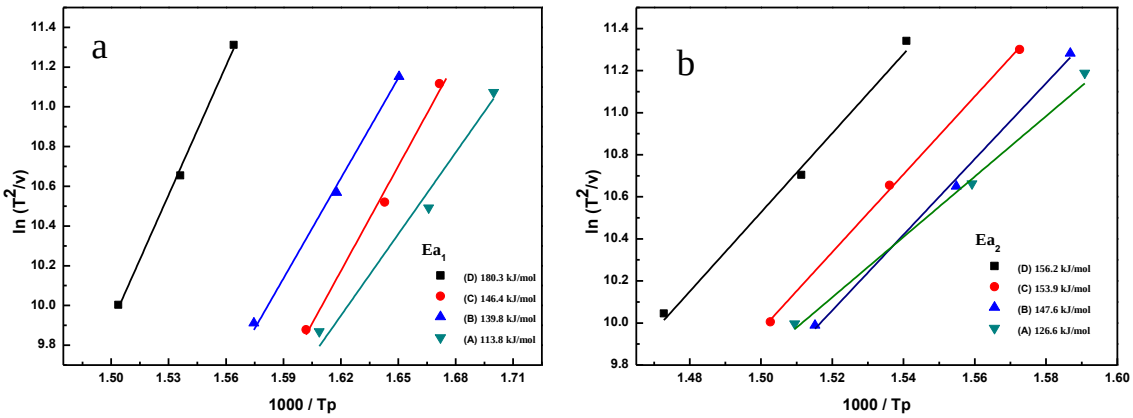

Figure 3. The relationship curves between $\ln({T_p}^2/\upsilon)$ and $(1000/T_p)$ for $NaMgH_3$ hydride and composites fitted by Kissinger method. (A) NH–2.5M–2.5G; (B) NH–5G; (C) NH–5M; (D) $NaMgH_3$ hydride (**a**) for the first decomposition step of $NaMgH_3$ hydride and (**b**) for the second decomposition step of $NaMgH_3$ hydride.

Table 1. Calculated value of ΔE of the decomposition of the $NaMgH_3$ hydride.

Sample	1st Step ΔE_1 (kJ/mol)	2nd Step ΔE_2 (kJ/mol)
NH–2.5M–2.5G	113.8	126.6
NH–5G	139.8	147.6
NH–5M	146.4	153.9
$NaMgH_3$ hydride	180.3	156.2

3.3. Dehydriding Kinetic Properties of $NaMgH_3$ Hydride and NH-CM Composites

The isothermal dehydriding properties of the four samples at different temperatures (593 K, 613 K, and 638 K) are shown in Figures 4–6, respectively. In comparison with $NaMgH_3$ hydride, all NH-CM composites present better dehydriding kinetic properties. The hydrogen-desorbed amount increases with the increase in temperature. Among these three NH-CM composites, the NH–2.5M–2.5G composite has the best catalytic effect in improving the dehydriding kinetic properties of the $NaMgH_3$ hydride, where 90% of the maximum theoretical capacity (3.64 wt. % hydrogen) is released within 20 min at 638 K. Table 2 shows the maximum amount of hydrogen desorbed from the $NaMgH_3$ hydride and the NH-CM composites at different temperatures. These results agree well with that observed in Figures 2 and 3, indicating that dehydriding kinetics and dehydriding temperatures can be effectively reduced by a combined catalytic addition of MWCNTs and GO.

Table 2. The maximum amount of hydrogen desorbed from $NaMgH_3$ hydride and NH-CM composites at different temperatures.

Sample/Temperature	593 K (wt. %)	613 K (wt. %)	638 K (wt. %)
$NaMgH_3$	1.13	2.03	3.42
NH–5M	1.36	2.46	3.40
NH–5G	1.21	2.49	3.64
NH–2.5G–2.5M	1.46	2.56	3.64

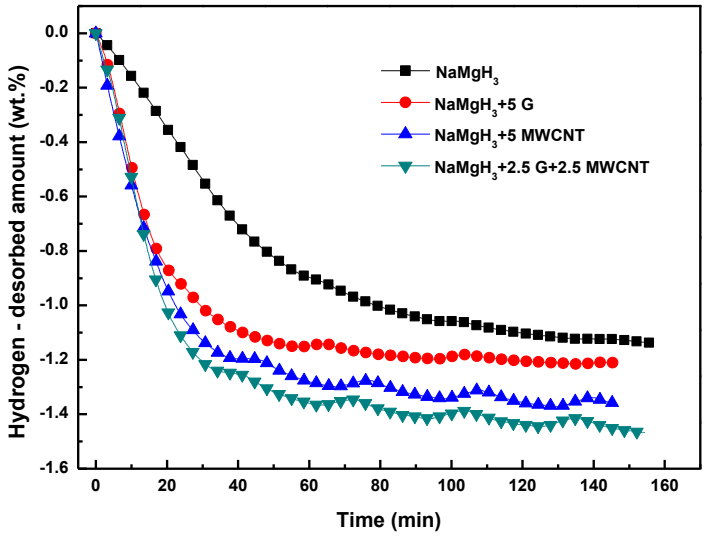

Figure 4. Dehydriding kinetic curves of the $NaMgH_3$ hydride and the NH-CM composites at 593 K.

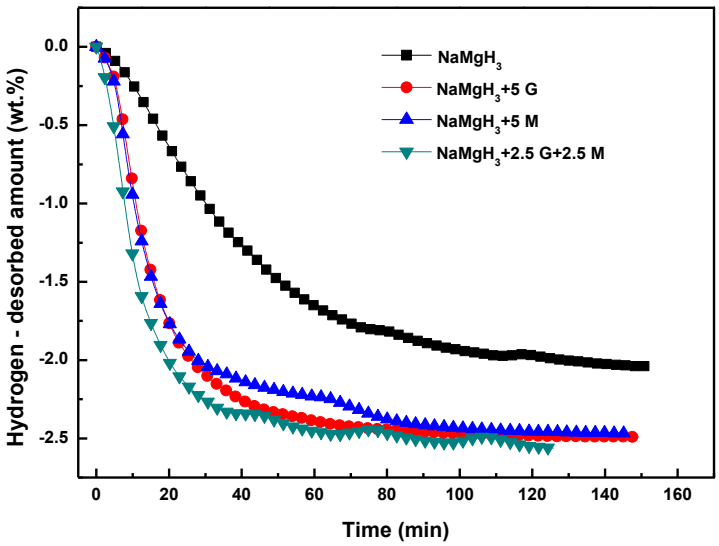

Figure 5. Dehydriding kinetic curves of the $NaMgH_3$ hydride and the NH-CM composites at 613 K.

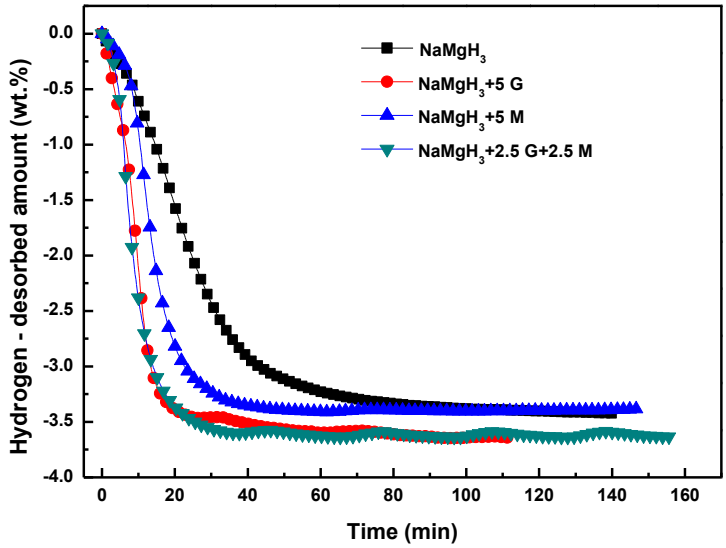

Figure 6. Dehydriding kinetic curves of the $NaMgH_3$ hydride and the NH-CM composites at 638 K.

To illustrate the decomposition mechanism of the NH-CM hydride composites, the XRD patterns of the $NaMgH_3$ + 2.5 G + 2.5 M sample after dehydriding at different temperatures are shown in Figure 7. With the increase in temperature from 593 K to 638 K, peaks of the $NaMgH_3$ phase become weakened, and peaks of the NaH phase and Mg phase become strengthened, such results agree well with our previous work for pristine $NaMgH_3$ hydride reported in [12]. In another word, the decomposition of $NaMgH_3$ is a two-step reaction: $NaMgH_3 \rightarrow NaH + Mg + H_2 \rightarrow Na + Mg + 3/2H_2$. The dopping with NM cannot change the decomposition process of $NaMgH_3$, but contribute to its dehydriding kinetics.

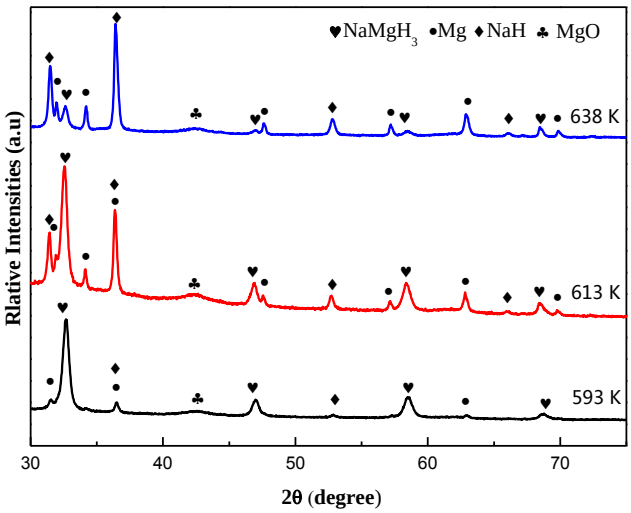

Figure 7. XRD patterns of $NaMgH_3$ + 2.5 G + 2.5 M hydride composite after dehydriding at different temperatures (593 K, 613 K, and 638 K).

One of the possible reasons for the enhancement of dehydriding kinetics of $NaMgH_3$ hydride is because of the ball milling process with CM additives, which creates more defects, a refined grain size, and a distorted crystal structure. Such structural features and observed improvements have also been reported in the case of the reactive ball milling of magnesium hydride with carbon additives in hydrogen gas [10,11,41–43]. A synergetic effect may exist in the NH–2.5M–2.5G composite, where the presence of MWCNTs may hinder the restacking of GO; hence, improving the dehydriding

kinetics. Bhatnagar et al. reported this synergetic effect in MgH_2–$NaAlH_4$ composite with the addition of 1.5 wt. % of graphene nanosheets and 0.5 wt. % of single wall carbon nanotube [45]. Further work is still needed to illustrate its possible mechanism.

4. Conclusions

$NaMgH_3$ perovskite hydride and NH-CM composites were prepared via the reactive ball-milling method under a H_2 atmosphere. MWCNTs and GO were used as a catalyst to improve the dehydriding kinetic properties of $NaMgH_3$ hydride. Dehydriding temperature and activation energy (ΔE) for two dehydrogenation steps of $NaMgH_3$ hydride can be greatly reduced with a 5 wt. % CM addition, especially the composite with a combined addition of 2.5 wt. % MWCNTs + 2.5 wt. % GO (NH–2.5M–2.5G). In comparison with $NaMgH_3$ hydride, the ΔE_1 and ΔE_2 of the NH–2.5M–2.5G composite are reduced by about 67 kJ/mol and 30 kJ/mol, respectively. The maximum amount of hydrogen desorbed is 3.64 wt. % at 638 K, and about 90% of the maximum amount was released within 20 min. This can be attributed to the synergetic effect between MWCNTs and GO, indicating that the combination of MWCNTs and GO is a better catalyst as compared to MWCNTs or GO alone.

Acknowledgments: This work was financially supported by the National Natural Science Foundation of China (51261003, 51471055) and the Guangxi Natural Science Foundation (2016GXNSFGA380001).

Author Contributions: Wang and Tao conceived and designed the study. Tao and Li performed the experiments. Deng provided the DSC analyses. Yao contributed significantly to XRD refinement and analysis; Wang wrote the manuscript. Zhou helped perform the analysis with constructive discussions. All authors read and approved the manuscript.

Conflicts of Interest: The authors declare no conflict of interest.

References

1. Bououdina, M.; Grant, D.; Walker, G. Review on hydrogen absorbing materials—Structure, microstructure, and thermodynamic properties. *Int. J. Hydrog. Energy* **2006**, *31*, 177–182. [CrossRef]
2. Pottmaier, D.; Pinatel, E.R.; Vitillo, J.G.; Garroni, S.; Orlova, M.; Baro, M.D.; Vaughan, G.B.M.; Fichtner, M.; Lohstroh, W.; Baricco, M. Structure and thermodynamic properties of the $NaMgH_3$ perovskite: A comprehensive study. *Chem. Mater.* **2011**, *23*, 2317–2326. [CrossRef]
3. Bouhadda, Y.; Fenineche, N.; Boudouma, Y. Hydrogen storage: Lattice dynamics of orthorhombic $NaMgH_3$. *Phys. B* **2011**, *406*, 1000–1003. [CrossRef]
4. Vajeeston, P.; Ravindran, P.; Kjekshus, A.; Fjellvag, H. First-principles investigations of the $MMgH_3$ (M = Li, Na, K, Rb, Cs) series. *J. Alloy. Compd.* **2008**, *450*, 327–337. [CrossRef]
5. Bouhadda, Y.; Boudouma, Y.; Fenineche, N.; Bentabet, A. Ab initio calculations study of the electronic, optical and thermodynamic properties of $NaMgH_3$, for hydrogen storage. *J. Phys. Chem. Solids* **2010**, *71*, 1264–1268. [CrossRef]
6. Wu, H.; Zhou, W.; Udovic, T.J.; Rush, J.J.; Yildirim, T. Crystal chemistry of perovskite-type hydride $NaMgH_3$: Implications for hydrogen storage. *Chem. Mater.* **2008**, *20*, 2335–2342. [CrossRef]
7. Bouhadda, Y.; Bououdina, M.; Fenineche, N.; Boudouma, Y. Elastic properties of perovskite-type hydride $NaMgH_3$ for hydrogen storage. *Int. J. Hydrog. Energy* **2013**, *38*, 1484–1489. [CrossRef]
8. Bouamrane, A.; Laval, J.P.; Soulie, J.P.; Bastide, J.P. Structural characterization of $NaMgH_2F$ and $NaMgH_3$. *Mater. Res. Bull.* **2000**, *35*, 545–549. [CrossRef]
9. Sheppard, D.A.; Paskevicius, M.; Buckley, C.E. Thermodynamics of hydrogen desorption from $NaMgH_3$ and its application as a solar heat storage medium. *Chem. Mater.* **2011**, *23*, 4298–4300. [CrossRef]
10. Ikeda, K.; Nakamori, Y.; Orimo, S. Formation ability of the perovskite-type structure in $Li_xNa_{1-x}MgH_3$ (x = 0, 0.5 and 1.0). *Acta Mater.* **2005**, *53*, 34–53. [CrossRef]
11. Martínez-Coronado, R.; Sánchez-Benítez, J.; Retuerto, M.; Fernández-Díaz, M.T.; Alonso, J.A. High-pressure synthesis of $Na_{1-x}Li_xMgH_3$ perovskite hydrides. *J. Alloy. Compd.* **2012**, *522*, 101–105. [CrossRef]
12. Wang, Z.; Li, J.; Tao, S.; Deng, J.; Zhou, H.; Yao, Q. Structure, thermal analysis and dehydriding kinetic properties of $Na_{1-x}Li_xMgH_3$ hydrides. *J. Alloy. Compd.* **2016**, *660*, 402–406. [CrossRef]

13. Tao, S.; Wang, Z.; Li, J.; Deng, J.; Zhou, H.; Yao, Q. Improved dehydriding properties of $NaMgH_3$ pervoskite hydride by addition of graphitic carbon nitride. *Mater. Sci. Forum* **2016**, *852*, 502–508. [CrossRef]
14. Li, Y.; Zhang, L.; Zhang, Q.; Fang, F.; Sun, D.; Li, K.; Wang, H.; Ouyang, L.; Zhu, M. In situ embedding of Mg_2NiH_4 and YH_3 nanoparticles into bimetallic hydride $NaMgH_3$ to inhibit phase segregation for enhanced hydrogen storage. *J. Phys. Chem. C* **2014**, *118*, 23635–23644. [CrossRef]
15. Chaudhary, A.; Paskevicius, M.; Sheppard, D.A.; Buckley, C.E. Thermodynamic destabilization of MgH_2 and $NaMgH_3$ using Group IV elements Si, Ge or Sn. *J. Alloy. Compd.* **2015**, *623*, 109–116. [CrossRef]
16. Webb, C.J. A review of catalyst-enhanced magnesium hydride as a hydrogen storage material. *J. Phys. Chem. Solids* **2014**, *84*, 96–106. [CrossRef]
17. Bogdanović, B.; Hartwig, T.H.; Spliethoff, B. The development, testing and optimization of energy storage materials based on the MgH_2-Mg system. *Int. J. Hydrog. Energy* **1993**, *18*, 575–589. [CrossRef]
18. Sakintuna, B.; Lamari-Darkrim, F.; Hirscher, M. Metal hydride materials for solid hydrogen storage: A review. *Int. J. Hydrog. Energy* **2007**, *32*, 1121–1140. [CrossRef]
19. Bogdanović, B.; Spliethoff, B. Active MgH_2-Mg-systems for hydrogen storage. *Int. J. Hydrog. Energy* **1987**, *12*, 863–873. [CrossRef]
20. Bobet, J.-L.; Akiba, E.; Nakamura, Y.; Darriet, B. Study of Mg-M (M = Co, Ni and Fe) mixture elaborated by reactive mechanical alloying—Hydrogen sorption properties. *Int. J. Hydrog. Energy* **2000**, *25*, 987–996. [CrossRef]
21. Reiser, A.; Bogdanović, B.; Schlichte, K. The application of Mg-based metal-hydrides as heat energy storage systems. *Int. J. Hydrog. Energy* **2000**, *25*, 425–430. [CrossRef]
22. Fakioğlu, E.; Yürüm, Y.; Veziroğlu, T.N. A review of hydrogen storage systems based on boron and its compounds. *Int. J. Hydrog. Energy* **2004**, *29*, 1371–1376. [CrossRef]
23. Alsabawi, K.; Webb, T.A.; Gray, E.M.; Webb, C.J. The effect of C_{60} additive on magnesium hydride for hydrogen storage. *Int. J. Hydrog. Energy* **2015**, *40*, 10508–10515. [CrossRef]
24. Imamura, H.; Takesue, Y.; Akimoto, T.; Tabata, S. Hydrogen absorbing magnesium composites prepared by mechanicalgrinding with graphite: Effects of additives on composite structures and hydriding properties. *J. Alloy. Compd.* **1999**, *293–295*, 564–568. [CrossRef]
25. Imamura, H.; Tabata, S.; Shigetomi, N.; Takesue, Y.; Sakata, Y. Composites for hydrogen storage by mechanical grinding ofgraphite carbon and magnesium. *J. Alloy. Compd.* **2002**, *330–332*, 579–583. [CrossRef]
26. Thiangviriya, S.; Utke, R. Improvement of dehydrogenation kinetics of $2LiBH_4$-MgH_2 composite by doping with activated carbon nanofibers. *Int. J. Hydrog. Energy* **2016**, *41*, 2797–2806. [CrossRef]
27. Kadri, A.; Jia, Y.; Chen, Z.; Yao, X. Catalytically enhanced hydrogen sorption in Mg-MgH_2 by coupling vanadium-based catalyst and carbon nanotubes. *Materials* **2015**, *8*, 3491–3507. [CrossRef]
28. Spassov, T.; Zlatanova, Z.; Spassova, M.; Todorova, S. Hydrogen sorption properties of ball-milled Mg-C nanocomposites. *Int. J. Hydrog. Energy* **2010**, *35*, 10396–10403. [CrossRef]
29. Rud, A.D.; Lakhnik, A.M. Effect of carbon allotropes on the structure and hydrogen sorption during reactive ball-milling of Mg-C powder mixtures. *Int. J. Hydrog. Energy* **2012**, *37*, 4179–4187. [CrossRef]
30. Huang, Z.G.; Guo, Z.P.; Calka, A.; Wexler, D.; Liu, H.K. Effects of carbon black, graphite and carbon nanotube additives on hydrogen storage properties of magnesium. *J. Alloy. Compd.* **2007**, *427*, 94–100. [CrossRef]
31. Mandzhukova, T.; Grigorova, E.; Khristov, M.; Tsyntsarski, B. Investigation of the effect of activated carbon and 3d-metalcontaining additives on the hydrogen sorption properties of magnesium. *Mater. Res. Bull.* **2011**, *46*, 1772–1776. [CrossRef]
32. Grigorova, E.; Mandzhukova, T.; Tsyntsarski, B.; Budinova, T.; Khristov, M.; Tzvetkov, P.; Petrova, B.; Petrov, N. Effect of activated carbons derived from different precursors on the hydrogen sorption properties of magnesium. *Fuel Process. Technol.* **2011**, *92*, 1963–1969. [CrossRef]
33. Wu, C.Z.; Wang, P.; Yao, X.; Liu, C.; Chen, D.M.; Lu, G.Q.; Cheng, H.M. Effect of carbon/noncarbon addition on hydrogen storage behaviors of magnesium hydride. *J. Alloy. Compd.* **2006**, *414*, 259–264. [CrossRef]
34. Wu, C.Z.; Wang, P.; Yao, X.; Liu, C.; Chen, D.M.; Lu, G.Q.; Cheng, H.M. Hydrogen storage properties of MgH_2/SWNT composite prepared by ball milling. *J. Alloy. Compd.* **2006**, *420*, 278–282. [CrossRef]
35. Skripnyuk, V.M.; Rabkin, E.; Bendersky, L.A.; Magrez, A.; Carreño-Morelli, E.; Estrin, Y. Hydrogen storage properties of as-synthesized and severely deformed magnesium multiwall carbon nanotubes composite. *Int. J. Hydrog. Energy* **2010**, *35*, 5471–5478. [CrossRef]

36. Schaller, R.; Mari, D.; dos Santos, S.M.; Tkalcec, I.; Carreño-Morelli, E. Investigation of hydrogen storage in carbonnanotube-magnesium matrix composites. *Mater. Sci. Eng. A* **2009**, *521–522*, 147–150. [CrossRef]
37. Singh, R.K.; Raghubanshi, H.; Pandey, S.K.; Srivastava, O.N. Effect of admixing different carbon structural variants on the decomposition and hydrogen sorption kinetics of magnesium hydride. *Int. J. Hydrog. Energy* **2010**, *35*, 4131–4137. [CrossRef]
38. Ranjbar, A.; Ismail, M.; Guo, Z.P.; Yu, X.B.; Liu, H.K. Effects of CNTs on the hydrogen storage properties of MgH_2 and MgH_2-BCC composite. *Int. J. Hydrog. Energy* **2010**, *35*, 7821–7826. [CrossRef]
39. Chen, B.-H.; Kuo, C.-H.; Ku, J.-R.; Yan, P.-S.; Huang, C.-J.; Jeng, M.-S.; Tsau, F.-H. Highly improved with hydrogen storage capacity and fast kinetics in Mg-based nanocomposites by CNTs. *J. Alloy. Compd.* **2013**, *568*, 78–83. [CrossRef]
40. Ikeda, K.; Kato, S.; Shinzato, Y.; Okuda, N.; Nakamori, Y.; Kitano, A.; Yukawa, H.; Morinaga, M.; Orimo, S. Thermodynamical stability and electronic structure of aperovskite-type hydride, $NaMgH_3$. *J. Alloy. Compd.* **2007**, *446–447*, 162–165. [CrossRef]
41. RÖnnebro, E.; Noréus, D.; Kadir, K.; Reiser, A.; Bogdanovic, B. Investigation of the perovskite related structures of $NaMgH_3$, $NaMgF_3$ and Na_3AlH_6. *J. Alloy. Compd.* **2000**, *299*, 101–106. [CrossRef]
42. Tao, S.; Wang, Z.; Deng, J.; Zhou, H.; Yao, Q. Improvement of dehydrogenation kinetics of $NaMgH_3$ hydride by introducing K_2TiF_6 as Dopant. *Int. J. Hydrog. Energy* **2016**, in press.
43. Reardon, H.; Mazur, N.; Gregory, D.H. Facile synthesis of nanosized sodium magnesium hydride, $NaMgH_3$. *Prog. Nat. Sci. Mater. Int.* **2013**, *23*, 343–350. [CrossRef]
44. Kissinger, H.E. Reaction kinetics in differential thermal analysis. *Anal. Chem.* **1957**, *29*, 1702–1706. [CrossRef]
45. Bhatnagar, A.; Pandey, S.K.; Dixit, V.; Shukla, V.; Shahi, R.R.; Shaza, M.A.; Srivastava, O. Catalytic effect of carbon nanostructures on the hydrogen storage properties of MgH_2–$NaAlH_4$ composite. *Int. J. Hydrog. Energy* **2014**, *39*, 14240–14246. [CrossRef]